



## Short communication

# Flash-sintering of $\text{Co}_2\text{MnO}_4$ spinel for solid oxide fuel cell applications

Andre L.G. Prette <sup>a,b</sup>, Marco Cologna <sup>b</sup>, Vincenzo Sglavo <sup>a</sup>, Rishi Raj <sup>b,\*</sup>

<sup>a</sup> Department of Materials Engineering and Industrial Technology, University of Trento, 38050 Trento, Italy

<sup>b</sup> Department of Mechanical Engineering, University of Colorado at Boulder, Boulder, CO 80309-0427, United States

## ARTICLE INFO

### Article history:

Received 16 August 2010

Received in revised form 9 October 2010

Accepted 14 October 2010

Available online 11 November 2010

### Keywords:

SOFCE

Spinel

Interconnect

Sintering

## ABSTRACT

We show that cobalt manganese oxide ( $\text{Co}_2\text{MnO}_4$ ) spinel can be sintered (without the application of external pressure) in a few seconds at about  $\sim 325^\circ\text{C}$  by applying a DC electrical field of  $12.5 \text{ V cm}^{-1}$ , by a process known as flash-sintering. A transition from normal to flash-sintering occurs when the field is  $\geq 7.5 \text{ V cm}^{-1}$ . The flash sintering phenomenon has also been observed in yttria-stabilized zirconia (3YSZ). Together, the results for 3YSZ and  $\text{Co}_2\text{MnO}_4$  point towards the generality of the process, since 3YSZ is an ionic conductor while the spinel is a predominantly electronic conductor. The  $\text{Co}_2\text{MnO}_4$  spinels are used to protect metals, such as stainless steels, in solid oxide fuel cells. The low temperatures employed in flash sintering can obviate interfacial interdiffusion with the metal substrate; in nominal sintering these interfacial reactions can produce deleterious interfacial phases.

© 2010 Elsevier B.V. All rights reserved.

## 1. Introduction

Interconnects are an important component in planar solid oxide fuel cells (SOFC). They are placed between the cathode and the anode of adjacent cells, thus carrying the current through the stack [1,2]. Ceramic interconnects based on perovskite structure of  $\text{LaCrO}_3$  are most commonly used in these applications. However, ceramic interconnects suffer from drawbacks [3,4]. Their cost is high (compared to metals), and they require high sintering temperatures ( $1450\text{--}1600^\circ\text{C}$ ). Samples sintered below  $1000^\circ\text{C}$  have low density and, therefore, poor electronic conductivity [3,4].

An alternative design for these interconnects is to use metals. However, metals must be protected against corrosion in oxidizing and reducing environments. Usually a ceramic coating is applied to the metal to achieve this protection. For example, stainless steel with high Cr is often used as the metal conductor since Cr helps to match the thermal expansion coefficient to that of other SOFC components [5]. However, chromium tends to migrate to the triple-phase boundary of the cathode [6], known as "poisoning". In order to reduce chromium poisoning, interconnects are coated with a protective oxide [1,7–11]. Open porosity in the coating must be avoided to prevent migration of chromium from the stainless steel to the cathode [7,8,12]. Cobalt manganese oxide spinels are commonly used as protective layers because they have high electronic conductivity, are stable in oxidizing atmospheres, and have a ther-

mal expansion coefficient close to stainless steel [1,10]. To obtain microstructures with closed pores in a conventional sintering process, temperatures of  $1100^\circ\text{C}$  or higher and dwell times of several hours are required [13]. At these temperatures chromium forms a brittle, and non-conducting chromium oxide interlayer with the stainless steel substrate [13]. Novel techniques known as field assisted sintering techniques [14–16], where pressure, electrical currents and microwaves are employed to enhance sintering, may be one of the ways to reduce the sintering temperature of Co–Mn–O spinel.

In recent work it has been shown that moderate DC electrical fields and currents can reduce the sintering temperature for tetragonal 3 mol% yttria stabilized zirconia (3YSZ) by several hundreds of  $^\circ\text{C}$ . Furthermore, sintering occurs in just a few seconds; hence the process has been called flash-sintering [17,18]. This phenomenon was explained by a slower rate of grain growth [19], and by Joule heating at grain boundaries from the electrical current passing through them. Potentially, flash sintering can reduce the sintering temperature of the Co–Mn–O spinel to a sufficient degree that interdiffusion, and thereby the deleterious interfacial phases are prevented from forming.

However,  $\text{Co}_2\text{MnO}_4$  spinel is a predominantly electronic conductor, while 3YSZ, where flash sintering has been shown to be viable [18], is an ionic conductor. The main purpose of the present study was to see whether or not flash-sintering is possible in a ceramic that is electronically conducting. As reported below, the spinel is shown to sinter at  $\sim 325^\circ\text{C}$ , well below the nominal sintering temperature, in just a few seconds. Because the spinel is more conductive than 3YSZ, the currents at the onset of flash sintering are greater, and the electrical fields somewhat lower in the spinel.

\* Corresponding author. Tel.: +1 303492 1029; fax: +1 303492 3498.

E-mail address: [rishi.raj@colorado.edu](mailto:rishi.raj@colorado.edu) (R. Raj).

## 2. Materials and methods

$\text{Co}_2\text{MnO}_4$  powder (particle size  $\sim 10 \mu\text{m}$ , with a specific surface area of  $3.3 \text{ m}^2 \text{ g}^{-1}$ ) was mixed with 3-wt% binder (B-1000, Duramax, Dow Chemical, USA), with excess water to achieve a homogeneous mixture. The mixture was air dried at  $85^\circ\text{C}$  for 24 h and ground in a mortar. The powder was pressed into dog-bone shaped specimens with a pressure of  $\sim 280 \text{ MPa}$ . These specimens had a green density of  $55.6 \pm 1.2\%$ . The gage section was 21 mm long, with a rectangular cross-section of  $3.27 \pm 0.02 \text{ mm} \times 1.10 \pm 0.08 \text{ mm}$ .

The procedure described in Ref. [18] was followed. Sintering was performed in a vertical tubular furnace. The sample was suspended with two thick platinum wires (0.25 mm diameter) that carried the current from the power supply to the sample. A second pair of thin wires (0.127 mm diameter), that did not draw any current, measured the voltage applied to the sample, as in the 4-point method. A constant voltage was applied through the thick wires, while the furnace temperature was increased at  $10^\circ\text{C min}^{-1}$ , up to  $1200^\circ\text{C}$ . The shrinkage was measured with a CCD camera (with optical filters), placed underneath the furnace [18]. The power to the applied field was supplied by Sorensen DLM 80-13. The current was measured with a Keithley 2000 digital multimeter and the voltage with a Keithley 6517B digital electrometer. The acquisition system, multimeter and electrometer, were connected to a computer for sampling and storing the data automatically, at a sampling rate of 10 Hz.

## 3. Results

A plot of the true (shrinkage) strain versus the temperature is shown in Fig. 1. Each experiment was conducted at a fixed applied voltage. The initial field applied to the samples is shown for each data set in Fig. 1. The shrinkage strain,  $\varepsilon$ , was calculated from  $\varepsilon = \ln(\ell/\ell_0)$ , where  $\ell$  is the time dependent length of the gage section and  $\ell_0$  is the initial gage length.

The results in Fig. 1 show two distinct regions of sintering behavior. When the applied electric field is below  $2.5 \text{ V cm}^{-1}$ , the sintering rate increases gradually with applied field in a manner resembling field assisted sintering or FAST [14–16]. However, above

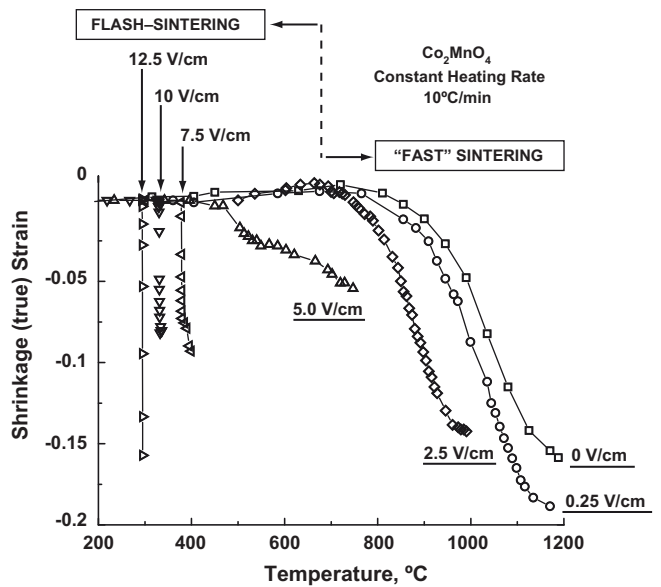


Fig. 1. Linear shrinkage at different levels of applied electrical fields as a function of furnace temperature. All experiments at constant heating rate of  $10^\circ\text{C min}^{-1}$ .

$7.5 \text{ V cm}^{-1}$  sintering occurs in a few seconds, characteristic of flash sintering [18]. The temperature for the onset of sintering decreases at higher fields. At a field of  $12.5 \text{ V cm}^{-1}$  sintering occurs at just above  $325^\circ\text{C}$ , which is a very low temperature for sintering this spinel.

(In the regime lying in between FAST sintering and flash-sintering, which occurs near  $5.0 \text{ V cm}^{-1}$ , the behavior was unusual. In several attempts at  $5.0 \text{ V cm}^{-1}$  the sample broke in a similar fashion, near the connection to the platinum electrode. This behavior appears to be peculiar to flash sintering in the  $\text{Co}_2\text{MnO}_4$  spinel, and remains unexplained.)

The sample sintered without electrical field (shown as  $0 \text{ V cm}^{-1}$ ), was heated up to  $1188^\circ\text{C}$ ; it did not sinter to full density and contained open porosity, as seen in the micrographs in Fig. 2. However, the samples sintered under an electrical field sintered to a much greater extent and appeared to be devoid of intercon-

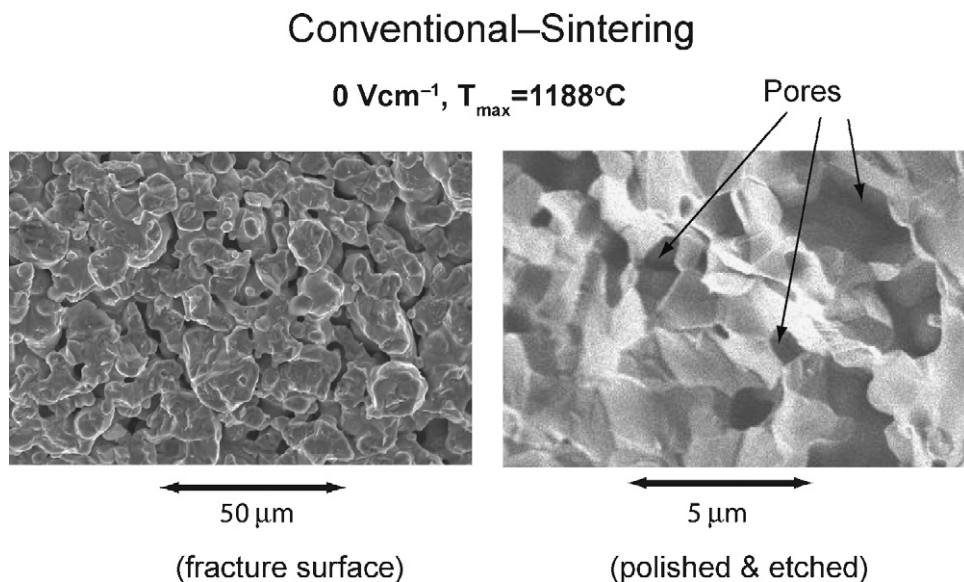
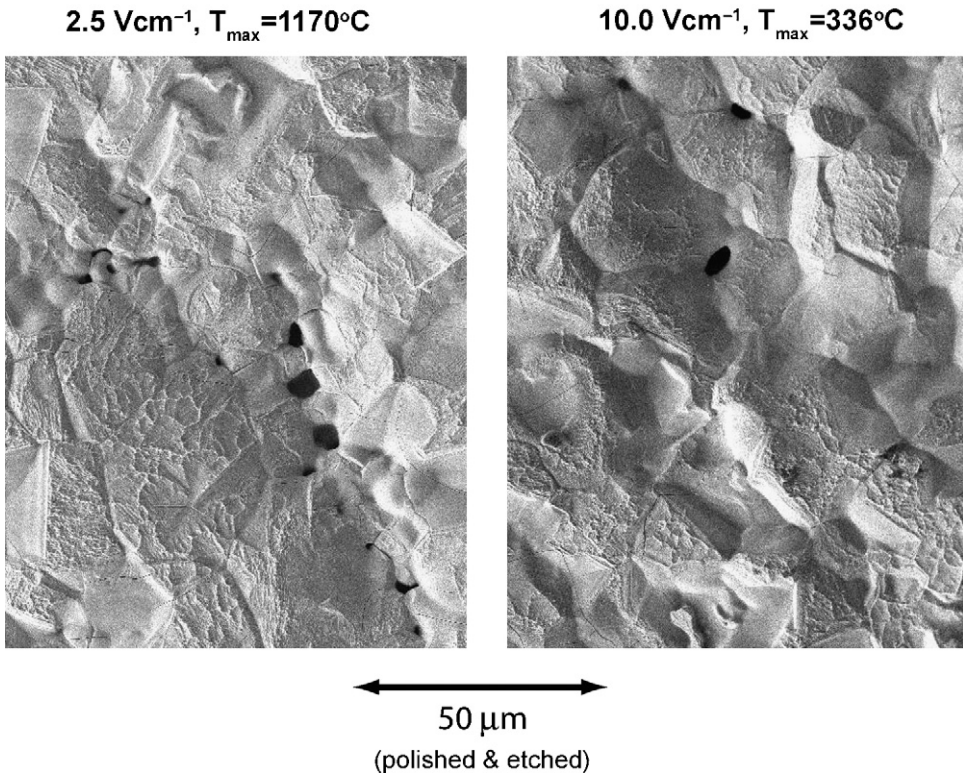


Fig. 2. Scanning electron micrographs (in secondary electron scattering mode) of the sample sintered without the application of electrical field ( $0 \text{ V cm}^{-1}$ ). The micrograph on the left shows the topology of a fracture surface of this specimen. The one on the right is obtained from a polished cross-section that has been thermally etched to reveal the grain boundaries.

## Flash–Sintering



**Fig. 3.** Scanning electron micrographs, taken in the secondary electron mode, of polished and thermally etched surfaces of samples at 0.25 V cm<sup>-1</sup> and 10 V cm<sup>-1</sup>.

nected pores. Micrographs of flash-sintered specimens are given in Fig. 3.

The X-ray diffraction spectra for the as received powder and the flash-sintered specimen (in this instance at a field of 12.5 V cm<sup>-1</sup>) are given in Fig. 4. The diffraction peaks from these two specimens are highly congruent, leading to the conclusion that the flash sintering process did not produce an intrinsic change in the structure of the spinel.

In the case of flash sintering ( $\geq 7.5 \text{ V cm}^{-1}$ , Fig. 1) sintering occurs almost instantly as seen by the nearly vertical slope of the shrinkage curves. The temperature to reach maximum density drops to  $\sim 400^\circ\text{C}$  at  $7.5 \text{ V cm}^{-1}$ , and to  $\sim 325^\circ\text{C}$  at  $12.5 \text{ V cm}^{-1}$ . The sintering rates, captured from CCD images taken 0.1 s apart, are plotted in Fig. 5. The sintering rates for FAST sintering, shown in the inset, are nearly 2 orders of magnitude slower than for flash-sintering.

Samples for SEM micrographs were prepared in two ways. The sample sintered without an electrical field (the 0 V cm<sup>-1</sup>), which contained significant porosity was fractured and the fracture surface examined in the SEM, as shown on the left in Fig. 2. In the other method the samples were cross-sectioned and polished and the surfaces were thermally etched by annealing at  $1150^\circ$  for 1 h, to delineate the grain boundaries. The grain boundaries in these micrographs are revealed by differences in the topography of the crystallites that are contained by them. The surfaces of the crystallites vary in their shape and depth because their etching rates vary with orientation. These micrographs obtained in secondary emission in the SEM are shown on the right in Fig. 2 (the 0 V specimen) and in Fig. 3 (the 2.5 V cm<sup>-1</sup> and 10.0 V cm<sup>-1</sup> specimen). A comparison of the micrographs in Figs. 2 and 3 show the high degree of interconnected porosity in the 0 V specimen but only a few isolated pores in the micrographs in Fig. 3 for the flash sintered specimens. The shape of the grains do not have any correlation with the direction of the applied electrical field, implying that the direction of the electrical current did not have an influence on the migration of the grain boundaries during sintering. Grain sizes were measured by the linear intercept method yielding values of  $17.9 \pm 0.2 \mu\text{m}$ ,  $18.3 \pm 0.1 \mu\text{m}$  and  $18.7 \pm 0.2 \mu\text{m}$ , respectively for 0 V cm<sup>-1</sup>, 0.25 V cm<sup>-1</sup> and 10 V cm<sup>-1</sup>.

An Arrhenius plot showing the power dissipation as function of temperature is shown in Fig. 6. The power was calculated from the product of the DC current passing through the sample and the voltage measured across the specimen with the thin platinum wires as explained earlier. Flash-sintering is characterized by the onset of a power-surge, that is not seen in the case of FAST sintering. It is interesting to note that the onset of flash-sintering occurs at a power level of about 1 W, similar to the observation made in flash-sintering of 3YSZ [18] (the specimen size was the same in both sets of experiments). However, the power dissipation rises very

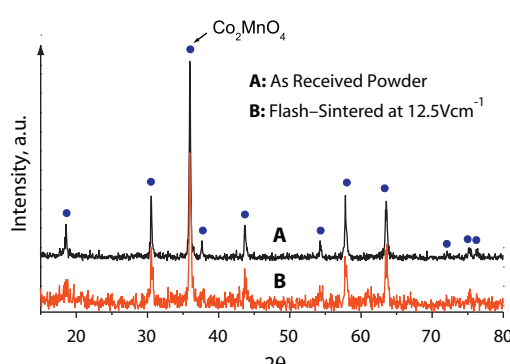


**Fig. 4.** X-ray spectra from as received spinel powder and the sample sintered at 12.5 V cm<sup>-1</sup>.

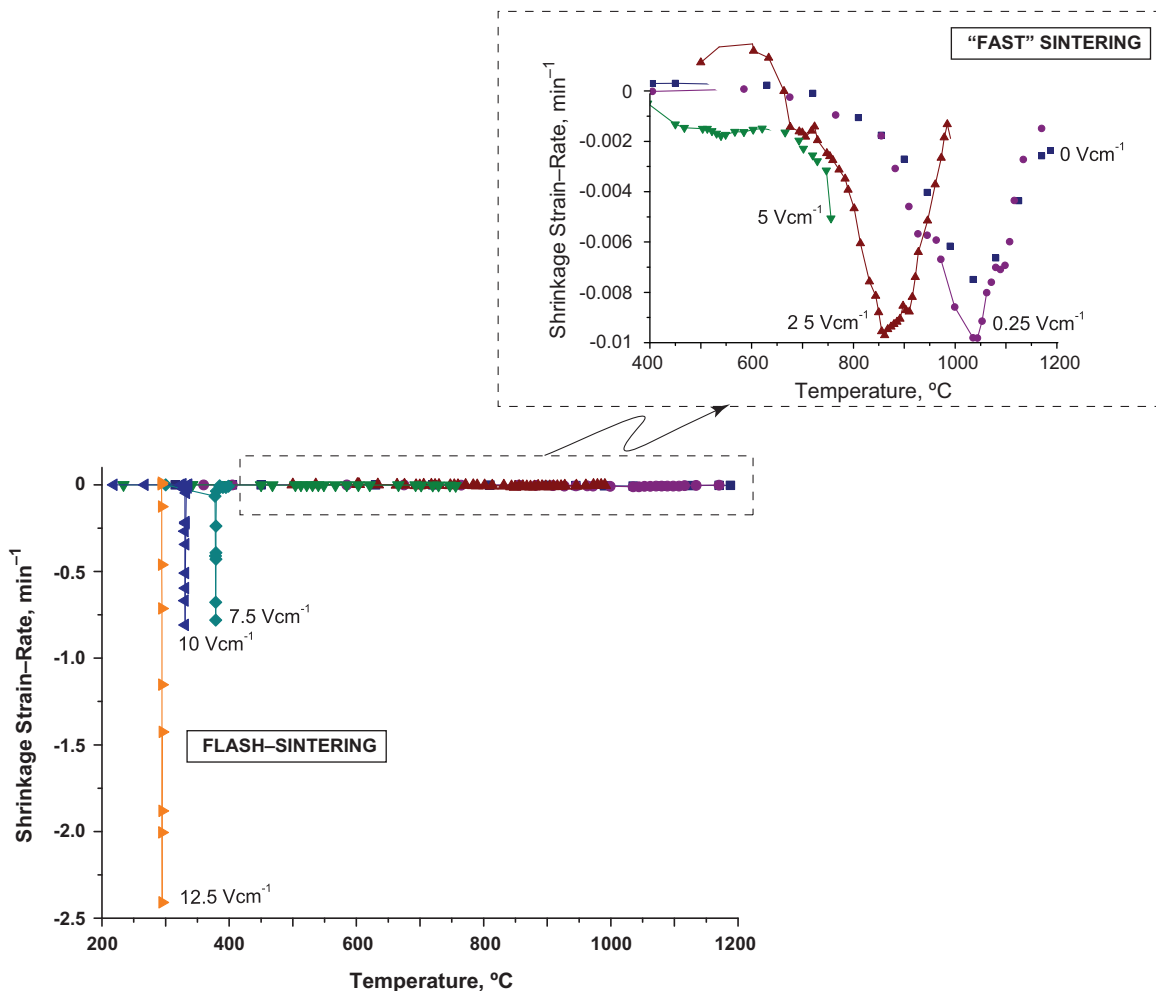


**Fig. 5.** Plots of shrinkage rates at different applied fields.

quickly in the present experiments, much more so than in the 3YSZ experiments because the spinel has higher conductivity. The upper limit in the current, and the corresponding voltage for the sintering experiments are listed in Table 1. It is not clear whether or not these high rates of power dissipation are needed for the completion of flash-sintering. The onset of flash-sintering begins at much lower power levels, about 1 W. Lacking equipment to limit the current immediately at the onset, that is at 1 W, we are unable to say whether or not the high power levels given in Table 1 are a necessary condition to achieve high sintered density.

#### 4. Discussion

In contrast with 3YSZ, which is an ionic conductor, flash sintering in  $\text{Co}_2\text{MnO}_4$ , which is a predominantly electronic conductor, occurs at a lower field and at lower temperatures. While 3YSZ required a field  $\geq 60 \text{ V cm}^{-1}$ ,  $\text{Co}_2\text{MnO}_4$  required only  $\geq 7.5 \text{ V cm}^{-1}$  to produce flash-sintering. The current in the spinel reached much higher levels than in 3YSZ. For example, in the case of 3YSZ experiments the circuit was designed to limit the current to 0.50 A, but this limit had to be increased to 13 A for the experiments with  $\text{Co}_2\text{MnO}_4$ .

The phenomenon of flash-sintering manifests itself as an instability in the power dissipation in the sample (keeping in mind that the experiments are carried out at a constant applied voltage). One explanation for this behavior is that grain boundaries, and particle-particle contacts, suffer local Joule heating, thereby

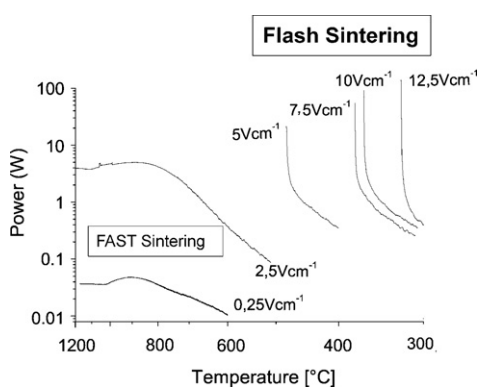


**Fig. 6.** Power dissipation in the sample as a function of temperature under different levels of applied electrical fields.

**Table 1**

The highest current, and the corresponding voltage measured in the sintering experiments.

Initial applied field ( $\text{V cm}^{-1}$ )	Measured voltage (V)	Maximum current (A)	Maximum power dissipation (W)
12.5	25	9.7	243
10	20	7.54	151
7.5	15	6.67	100
5	10	4.48	45
2.5	5	2.48	12
0.25	0.5	0.25	0.125

raising the rate of diffusional transport [18]. The argument is that power dissipation is localized at particle–particle junctions and grain boundaries because their electrical resistance is far greater than that of the grain matrix. This effect is especially pronounced in the early stages of sintering where the small contact area at particle–particle interfaces raises the local resistance and hence the temperature, thereby precipitating flash-sintering effect.

## 5. Conclusions

In conventional sintering, neck growth in  $\text{Co}_2\text{MnO}_4$  begins at about  $800^\circ\text{C}$ , and full densification is achieved at temperatures near  $1300^\circ\text{C}$  [13] in several hours. We show that application of modest DC electrical fields of  $12.5 \text{ V cm}^{-1}$ , lowers the sintering temperature to  $\sim 325^\circ\text{C}$ , and the sintering time to just a few seconds. At lower fields the sintering rate increases gradually with the applied field, similar to the phenomenon known as field assisted sintering (FAST). The sintering rates in flash-sintering are nearly two orders of magnitude faster than in FAST sintering, despite the much lower sintering temperatures. It is postulated that higher electrical resistance of grain boundaries and particle–particle contacts concentrates the power dissipation at interfaces, thereby producing a giant increase in the rate of diffusional transport.

A second distinction between flash and FAST sintering appears to lie in the grain growth behavior. In the case of 3YSZ, FAST sintering could be explained by the reduced rate of grain growth under an applied field [19]. However, here, in the case of  $\text{Co}_2\text{MnO}_4$ , the grain size is not significantly reduced, indeed it appears to be somewhat enhanced, suggesting the need to consider new mechanisms for this phenomenon.

Flash-sintering of  $\text{Co}_2\text{MnO}_4$  spinel is a compelling result for the fabrication of SOFC systems since it will prevent the formation of oxide interlayer between the spinel and the stainless steel that occurs during conventional sintering. However, experimental designs for implementing electrical fields and managing large currents during the sintering process will need to be developed. One possibility is to have a travelling electrode that moves on the sur-

face of the coating as it sinters, while the stainless steel substrate serves as the second electrode. While the power surges appear to be large, the ambient temperature for the sintering can be reasonably low to implement such a concept.

## Acknowledgements

This research was supported by the Basic Energy Sciences Division of the Department of Energy under Grant No.: DE-FG02-07ER46403. The materials for this study were provided by SOFC-Power, Trento, Italy. One of us, ALGP, wishes to acknowledge financial support from the Graduate School of the University of Trento.

## References

- [1] A. Petric, H. Ling, *J. Am. Ceram. Soc.* 90 (2007) 1515–1520.
- [2] Z. Yang, *Int. Mater. Rev.* 53 (2008) 39–54.
- [3] F. Tietz, H.-P. Buchkremer, D. Stover, *Solid State Ionics* 152–153 (2002) 373–381.
- [4] W. Zhu, M. Yan, *J. Zhejiang Univ. Sci. B* 5 (2004) 1471–1503.
- [5] J.Y. Kim, N.L. Canfield, L.A. Chick, K.D. Meinhardt, V.L. Sprengle, *Ceram. Eng. Sci. Proc.* 26 (2005) 129–138.
- [6] S.C. Paulson, V.I. Birss, *J. Electrochem. Soc.* 151 (2004) A1961–A1968.
- [7] M. Bertoldi, T. Zandonella, D. Montinaro, A. Quaranta, V.M. Sgavero, *Proc. European Fuel Cell Forum 2006*, Lucerne (CH), 2006.
- [8] M. Stanislowski, J. Froitzheim, L. Niewolak, W.J. Quadakkers, K. Hilpert, T. Markus, L. Singheiser, *J. Power Sources* 164 (2007) 578–589.
- [9] X. Chen, P.Y. Hou, C.P. Jacobson, S.J. Visco, L.C. De Jonghe, *Solid State Ionics* 176 (2005) 425–433.
- [10] A. Ballanda, P. Gannon, M. Deibert, S. Chevalier, G. Cabochea, S. Fontanara, *Surf. Coat. Technol.* 203 (2009) 3291–3296.
- [11] P. Piccardo, R. Amendola, S. Fontana, S. Chevalier, G. Caboche, P. Gannon, *J. Appl. Electrochem.* 39 (2009) 545–551.
- [12] M.C. Tucker, H. Kurokawa, C.P. Jacobson, L.C. De Jonghe, S.J. Visco, *J. Power Sources* 160 (2006) 130–138.
- [13] A.L.G. Prette, V.M. Sgavero 33rd, *Int. Conf. Adv. Cer. Comp.*, Daytona, USA, 2008.
- [14] R. Orru', R. Licheri, A.M. Locci, A. Cincotti, G. Cao, *Mater. Sci. Eng. B* 63 (2009) 127–287.
- [15] Z.A. Munir, U. Anselmi-Tamburini, *J. Mater. Sci.* 41 (2006) 763–777.
- [16] S. Grasso, Y. Sakka, G. Maizza, *Sci. Technol. Adv. Mater.* 10 (2009) 053001.
- [17] Di Yang, R. Raj, H. Conrad, *J. Am. Ceram. Soc.* 93 (2010) 2935.
- [18] M. Cologna, B. Rashkova, R. Raj, *J. Am. Ceram. Soc.* (2010), doi:10.1111/j.1551-2916.2010.04289.x.
- [19] S. Ghosh, A.H. Chokshi, P. Lee, R. Raj, *J. Am. Ceram. Soc.* 92 (2009) 185.